Asian Journal of Chemistry; Vol. 36, No. 12 (2024), 2931-2938

ASIAN JOURNAL OF CHEMISTRY

https://doi.org/10.14233/ajchem.2024.32874

Entropy Driven Binding of 2-(4-Aminophenyl)benzothiazole with DNA: An Experimental and Theoretical Insights

RAGAIAHGARI SRINIVAS REDDY[1,2], BIJAYA KETAN SAHOO[1,*], ANNA TANUJA SAFALA BODAPATI[3], SHRAVYA RAO MADKU[1,4] and KANDIKONDA LAVANYA[1,5]

[1]Department of Chemistry, GITAM School of Science, GITAM Deemed to be University, Hyderabad Campus, Rudraram-502329, India
[2]Department of Chemistry, B.V. Raju Institute of Technology, Narsapur, Hyderabad-502313, India
[3]Chemistry Division, Basic Science & Humanities Department, BVRIT Hyderabad, College of Engineering for Women, Hyderabad-500090, India
[4]Department of Chemistry, St. Francis College for Women, Hyderabad-500016, India
[5]Department of Chemistry, Gouthami Institute of Technology and Management for Women, Proddatur-516360, India

*Corresponding author: E-mail: bsahoo@gitam.edu

Received: 12 October 2024; *Accepted*: 14 November 2024; *Published online*: 30 November 2024; AJC-21837

Molecular recognition driven by molecular interactions is an intricate part of drug discovery and targeted drug delivery systems due to the dependence of thetherapeutic properties of drugs on interaction with desired target biomolecules as receptors. 2-(4-Aminophenyl) benzothiazole (APB), a heterocyclic molecule containing a benzothiazole nucleus, is known to induce apoptosis besides inhibiting cancer cell development and has been found effective against different microorganisms. This study highlights the spectroscopic and theoretical investigation of binding interactions of APB and *ct*-DNA. The UV-vis experiments indicate a binding constant of $9.73 \pm 0.4 \times 10^5$ M^{-1}. The measured binding constants of $1.0 \pm 0.2 \times 10^5$, $2.4 \pm 0.3 \times 10^5$ and $3.5 \pm 0.3 \times 10^5$ at 298, 303 and 308 K, respectively, from fluorescence experiments indicated a dynamic quenching type. The binding was driven by hydrophobic forces with positive ΔH^o (64.8467 ± 2 KJ mol^{-1}) and ΔS^o (317.12 ± 2 J mol^{-1} K^{-1}) values besides spontaneity of the process with negative ΔG^o values. The binding of APB molecule in the minor groove of *ct*-DNA was demonstrated by DNA melting tests, viscosity measurements and site marker displacement using ethidium bromide and Hoechst. Additional studies conducted by KI provided support for minor groove binding and NaCl has no impact on the binding electrostatic interactions, while the CD investigations showed no DNA structural alterations. Molecular docking studies also confirmed the experimental findings placing APB in the *ct*-DNA minor groove.

Keywords: Benzothiazole, DNA, Fluorescence, Circular dichroism, Binding constant, Molecular docking.

INTRODUCTION

Benzothiazole and its derivatives have various pharmacological activity, including significant antibacterial and antifungal effects, with certain derivatives being effective against treatment of resistant microorganisms [1]. Studies have shown that these derivatives can effectively block critical inflammation-related processes [2]. In addition, several specific benzothiazole compounds have demonstrated potential in cancer research by displaying cytotoxic effects on different cancer cells [3]. Still, further research is required to fully understand the therapeutic potential, pharmacokinetics and toxicity of these compounds [4]. Recent research has shown that changing the benzothiazole structure can improve its effectiveness in biological activity and may open the possibilities for creating more potent drugs [5].

2-(4-Aminophenyl)benzothiazole (APB) highlights its extensive uses and biological functions [6-10]. Mavroidi *et al.* [11] highlighted APB compound promising use as a fluorescent probe specifically in biological imaging. Similarly, Li *et al.* [12] explored the interaction of this molecule with different biological targets, uncovering its potential as a versatile therapeutic agent. Sharma *et al.* [13] examined the structural modifications for enhancing its pharmacological properties whereas the stability of compound and its impact in the drug formulation has been reported by Kiritsis *et al.* [14].

Research on drug-DNA interactions is crucial for gaining insights into the molecular mechanisms of drug action and for developing safer and more targeted stimulants that specifically interact with DNA [15,16]. The crucial function of DNA in life processes, along with the biological potential of APB, prompted us to investigate their binding behaviour at the molecular level. This investigation used *ct*-DNA as the model biomolecule and the binding strength has been examined using fluorescence and UV-visible spectroscopy techniques. DNA melting and viscosity measurement, along with site marker investigations, have also been employed to ascertain the binding mechanism. To further understand the orientation of APB in *ct*-DNA, theoretical docking simulations were also run.

EXPERIMENTAL

The *ct*-DNA and ethidium bromide (EB), among other analytical reagents, from SRL India, whereas Sigma-Aldrich provided both 2-(4-aminophenyl)benzothiazole (APB) and Hoechst (HST). Absolute ethanol and phosphate buffer were used to prepare APB and *ct*-DNA stock solutions. The protein-free nature of the *ct*-DNA working solution was confirmed by an absorption ratio (A_{260}/A_{280}) of 1.8 [17-19]. Concentration of *ct*-DNA was ascertained in the solution by UV-vis spectrophotometry at 260 nm using a molar extinction coefficient of 6600 M^{-1} cm^{-1}. A 10 mM phosphate buffer containing 25 mM NaCl solution with a pH of 7.0 was used. Double-distilled water was used throughout the experiments while ensuring ethanol concentrations remained below 5%, which did not impact the system's operation.

Characterization: A Shimadzu double-beam spectrophotometer (model 1800) was employed to record the UV-vis absorption spectra using a 1 cm quartz cuvette. A Hitachi fluorescence spectrophotometer (F-2700) was used to record the fluorescence emission spectra. A slit width of 10 nm each for excitation and emission monochromator was set. A Jasco spectropolarimeter (J-810) was employed to measure the CD spectra at ambient temperature using a 2 mm quartz cell under a nitrogen atmosphere. A titration included adding APB to a predetermined concentration (200 µM) of *ct*-DNA, aiming for a molar ratio ([APB]/[ct-DNA]) between 0.5 and 1.5. Spectra were obtained by scanning from 220-330 nm at 100 nm/min.

Viscosity measurement: In this work, viscosity at 30 ºC was measured using an Ostwald viscometer [20-22]. The APB and *ct*-DNA mixture was incubated before the measurement. The samples were prepared by varying APB concentration from 0 to 100 µM and retaining *ct*-DNA concentration at 100 µM, resulting in a final 1:1 molar ratio. The flow time was recorded for the prepared samples and the average flow time for each data point was also computed from three runs.

DNA melting measurements: The DNA melting investigations were performed under thermostatic conditions using the UV-vis spectrophotometer. The experiment measured the absorbance of pure *ct*-DNA and its complex with APB from 30 to 90 ºC. The samples were prepared and incubated for 20 min before measurement. The experiment started with a 50 µM pure *ct*-DNA solution, followed by an equimolar 50 µM combination of APB and *ct*-DNA. For each value, three measurements were averaged.

Molecular docking: In this work, Auto Dock 4 was used for molecular docking studies. The crystal structure of B-DNA was generated from PDB with ID 453D. The 3D structure of APB molecule was obtained from PubChem and Open Babel translated the SDF file to the pdbqt file. After eliminating the water molecules, the DNA was added with polar hydrogen atoms and Kollman charges. The docking file of APB molecule was prepared following the docking protocol. The DNA-APB docking study was conducted using a free docking model with Auto-Dock 4.2.6′s Lamarckian Genetic Algorithm, after positioning the DNA within a grid of 0.375 Å. The remaining Auto Dock Program docking parameters were defaulted. Discovery Studio and PDBsum LIGPLOT [23] were used to interpret the Auto Dock results.

RESULTS AND DISCUSSION

UV-vis studies: The UV-vis absorption spectroscopy is often used to study DNA-small molecule interactions [23]. Three binding mechanisms are usual for interaction of small compounds and DNA. These interactions consist of groove binding, particularly in the minor groove, intercalation between base pairs and electrostatic binding external to the DNA helix. Intercalators show a red-shift of roughly 10 nm owing to their hypochromic action, whereas minor groove binders may have hyperchromicity with slight spectral shift [22,24,25]. When compared to groove binding, the effects of external binding are also comparable to those determined. The addition of *ct*-DNA changed the APB absorption behaviour (Fig. 1), where a decrease in the absorbance is observed in the presence of *ct*-DNA without any visible spectral shift. This spectral behaviour indicates an absence of intercalation mode and suggests groove or external interactions. The double reciprocal equation 1 (eqn. 1) was used to get the binding constant (K_a) [17]:

$$\frac{1}{\Delta A} = \frac{1}{(\varepsilon_b - \varepsilon_f)L_T} + \frac{1}{(\varepsilon_b - \varepsilon_f)L_t K_a}\frac{1}{M} \quad (1)$$

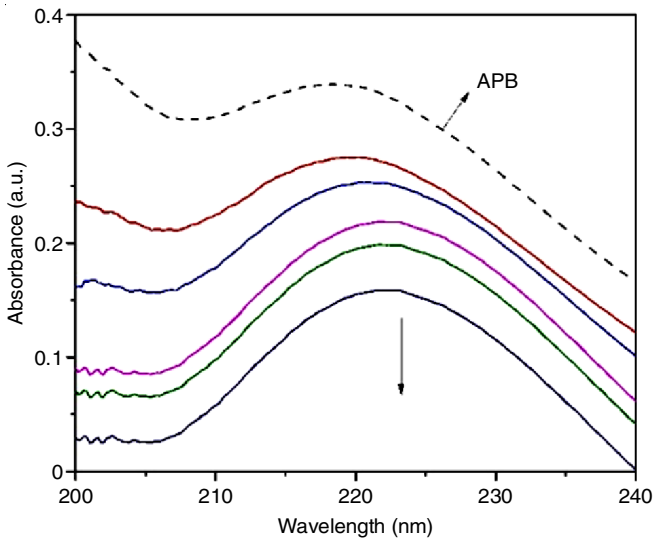

Fig. 1. Absorption behaviour of APB (10 µM, dotted line) in presence of increasing *ct*-DNA concentration

In eqn. 1, the molar extinction coefficients ε_b and ε_f represent the bound and free states, respectively; L_T and M are APB and *ct*-DNA concentrations. K_a value of $9.73 \pm 0.4 \times 10^5$ M^{-1} was calculated by dividing the intercept by the slope ($R^2 = 0.988$) obtained from the plot of 1/ΔA and 1/[*ct*-DNA] [26].

Quenching analysis: Mixed-type quenching involves both static and dynamic processes. Lifetime and temperature studies help differentiate the dynamic and static quenching processes. Increasing temperature has little effect on static quenching and a visible effect on dynamic quenching by increasing the dynamic quenching constant [27-30]. The quantitative property of the observed quenching was examined using eqn. 2 [31-33]. The Stern-Volmer constant K_{sv} can be calculated from the slope of the F_0/F against the [Q] graph.

$$\frac{F_0}{F} = 1 + K_{SV}[Q] = \frac{F_0}{F} = 1 + [Q]\,kq\,\tau_0 \quad (2)$$

where F_0 is the fluorescence intensity of APB; F is the fluorescence intensity with quencher *ct*-DNA; [Q] is the quencher concentration (*ct*-DNA); K_{sv} is the Stern-Volmer constant; kq is the bimolecular quenching constant; τ_0 is the fluorophore lifetime without the quencher; kq can be determined using eqn. 3 following the typical lifetime of a fluorophore in its excited state, which is 10^{-8} s [29].

$$K_{sv} = kq\,\tau_0 \quad (3)$$

As *ct*-DNA was gradually added, the fluorescence intensity of APB reduced without any change in the emission maxima, as observed in Fig. 2. The quenching constant of the observed fluorescence quenching at 298, 303 and 308 K was obtained using Stern-Volmer equation (eqn. 2) and tabulated in Table-1,

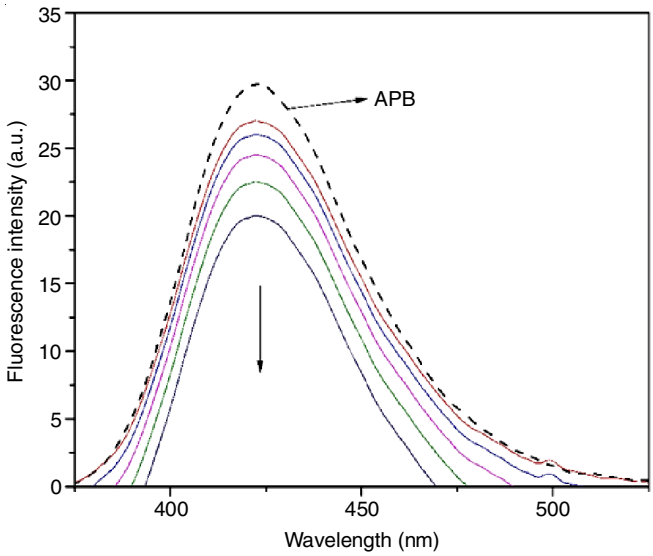

Fig. 2. Fluorescence emission spectra of pure APB (1 µM, dotted spectra) and in the presence of incremental (0-10 µM) *ct*-DNA (solid spectra)

whereas eqn. 3 was used to calculate the kq values. At higher temperatures, higher K_{SV} values suggested a dynamic quenching mechanism.

Binding analysis: Eqn. 4 was used to calculate the binding constant (K_b) and number of binding sites (n) [29]:

$$\log\frac{F_0 - F}{F} = \log K_b + n\log[Q] \quad (4)$$

where F and F_0 is the amount of fluorescence of APB with and without *ct*-DNA; [Q] is the concentration of unbound ligand at equilibrium. The double logarithmic plot at 298, 303 and 308 K is shown in Fig. 3 and found that the binding constant increased as the temperature rose (Table-1).

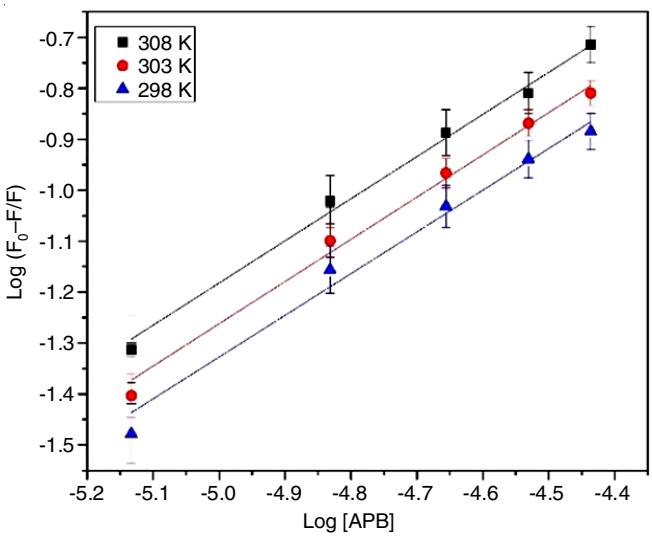

Fig. 3. Fluorescence quenching investigation at 298, 303 and 308 K

It is possible to attribute the increase in the binding constant with increasing temperature to the binding's endothermic activity (positive ΔH_0) [34]. The binding constant may increase with increasing temperature since the interacting species may diffuse more effectively at higher temperatures. The diffusion of molecules can be enhanced by increasing their velocities through elevated temperatures.

Interaction forces for APB-DNA binding system: The thermodynamic parameters were determined by fitting the binding constant values at different temperatures using van't Hoff's equation (eqn. 5):

$$\ln K_b = -\frac{\Delta H^\circ}{RT} + \frac{\Delta S^\circ}{R} \quad (5)$$

where the conventional changes in enthalpy and entropy are denoted by ΔH° and ΔS°, respectively; K_b stands for the binding constant; R is the gas constant and T is the absolute temperature (K). The ΔH° and ΔS° were determined using the regression

TABLE-1
BINDING AND THERMODYNAMIC PARAMETERS OF APB-DNA SYSTEM

Temp. (K)	K_b ($M \times 10^5$)	n	R^2	kq ($s\,M \times 10^{12}$)	K_{sv} ($M \times 10^5$)	ΔH°	ΔS°	ΔG°
298	1.0 ± 0.3	0.92	0.98	1.68 ± 0.2	1.68 ± 0.2	64.8467 ± 2	317.120 ± 2	-29.5286708 ± 1.5
303	2.4 ± 0.3	0.94	0.98	2.28 ± 0.2	2.28 ± 0.2			-31.6848516 ± 1.5
308	3.5 ± 0.3	0.95	0.97	3.40 ± 0.2	3.40 ± 0.2			-32.6892516 ± 1.5

equation's slope and intercept in the van't Hoff plot (Fig. 4). Using eqn. 6, the change in Gibbs free energy (ΔGº) was also determined.

$$\Delta G^\circ = -RT \ln K_b \quad (6)$$

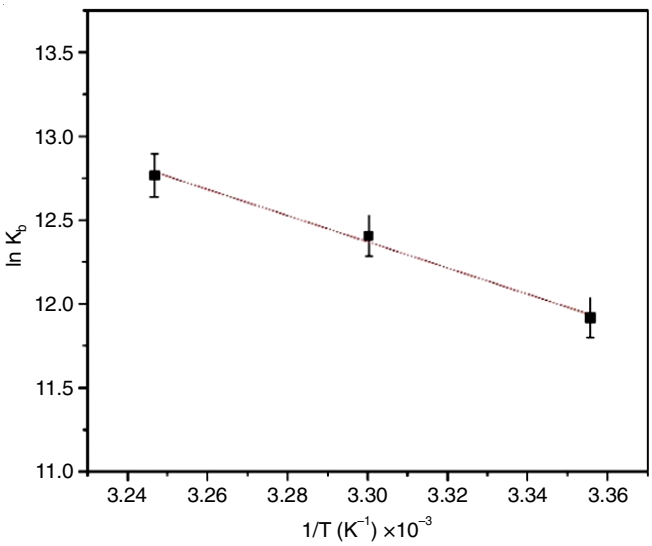

Fig. 4. van't Hoff plot of APB-HSA binding system

A negative Gibbs free energy change (ΔG°) suggests binding spontaneity, whereas the positive values for ΔH° and ΔS° indicate that hydrophobic forces dominate the binding process, driven by entropy over the enthalpy (Table-1).

Mode of the binding: The 3D structure of DNA nucleotide strands is right-handed helical.The minor and major grooves of DNA are formed by the stacking of base pairs and the helical twisting of the two strands around the axis. The intercalated zone is the region between base pairs. Minor groove binders are crescent-shaped, whereas intercalators are planar molecules that enter between the base pairs. Competitive displacement experiments reveal the DNA drug binding preferences. Fluorescence spectroscopy and DNA markers (ethidium bromide, Hoechst) were used to perform competitive displacement tests to determine binding mechanism of APB with *ct*-DNA [35].

Ethidium bromide (EB) displacement: Pure EB fluorescence brighter when bound to DNA [36-40]. Competing intercalating molecules may displace bound ethidium bromide from DNA, reducing its fluorescence intensity. Ethidium bromide (EB) fluorescence emission spectra with and without *ct*-DNA and with and without APB on DNA-bound EB are shown in Fig. 5, which shows no significant displacement of EB by APB, suggesting no intercalation. Thus, APB might attach outside or in the minor groove.

Displacement of Hoechst 33258: The primary method of investigation of minor groove binding mode [18] is the HST displacement. Pure HST is only moderately fluorescent but becomes quickly brighter when attached to DNA. A molecule that competes with HST for the minor grooves inside of DNA when introduced, replaces HST. The competitive displacement of HST by the competing molecule will lower the fluorescence intensity of bound HST. The competitive displacement of HST

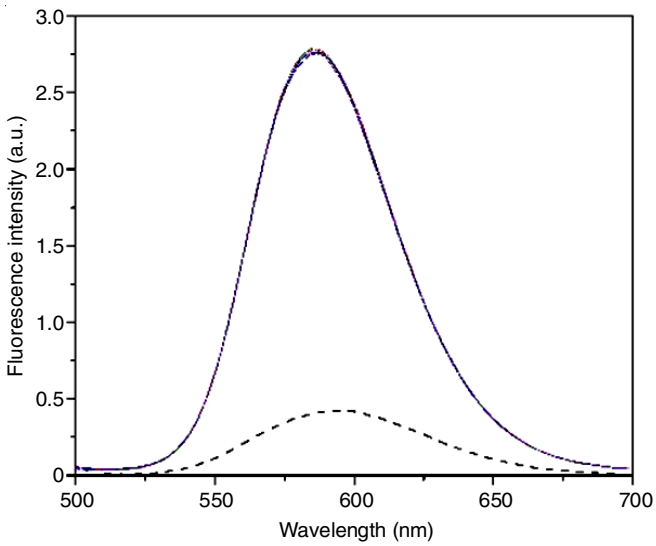

Fig. 5. Emission spectra of EB (1 μM) with the addition of APB (0-10 μM). in the presence (solid line) and absence of *ct*-DNA (dotted line)

by APB is shown in Fig. 6. The fluorescence intensity of HST was poor when it was in its pure form (dotted spectra), but the fluorescence intensity was increased by *ct*-DNA (top solid spectra). APB displaced the bound HST from ct-DNA, resulting in a decrease in the intensity of the bound HST and confirms the binding of APB in DNA minor groove.

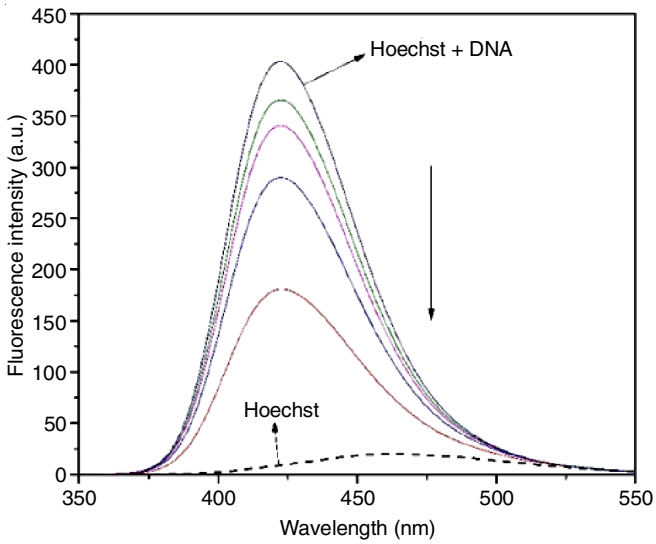

Fig. 6. Emission spectra of Hoechst (1 μM) in the absence of *ct*-DNA and with the addition of *ct*-DNA (0-10 μM), the downward arrow represents a decrease in intensity of Hoechst with the addition of APB

Circular dichroism (CD) studies: Drugs may alter DNA conformation that can be observed by the CD spectral patterns. The CD spectrum of DNA shows a positive peak at 275 nm for base stacking and a negative peak at 245 nm for right-handed B-DNA helicity [41-43]. Depending on the pharmacological interactions, these bands may stabilize or destabilize DNA [44,45]. Intercalation with small molecules alters the DNA structure [46,47], whereas groove binders do not. The CD spectrum of natural *ct*-DNA and in presence of APB is shown in Fig. 7, where the positive peak at 275 nm and the negative

peak at 245 nm showed *ct*-DNA's natural B-form conformation. APB did not modify the spectrum (peak position), indicating that *ct*-DNA stays in the B-form. The distinctive bands of DNA as observed in Fig. 7 (dotted spectra) illustrate its original conformation. The lack of observable peak shift after the interaction indicates the absence of binding induced conformational changes in DNA. The observed circular dichroism characteristic of the interaction indicates the lack of intercalation and suggests a groove-binding mechanism.

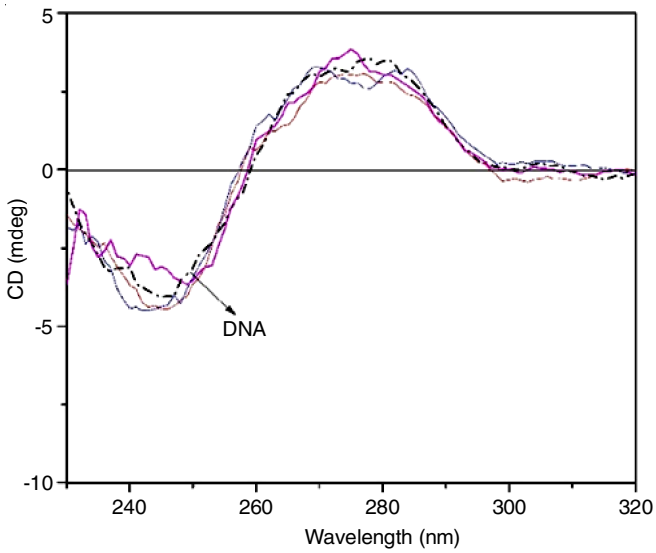

Fig. 7. CD spectra of DNA (200 µM) in the presence of APB; [APB]/[DNA] = 0.5-1.5

DNA melting investigations: The mechanism of APB binding to DNA was studied using DNA melting [48-50]. UV-vis spectroscopy measured DNA melting by measuring the absorbance of *ct*-DNA and its 1:1 combination with APB at 30-90 ºC. DNA melting breaks hydrogen bonds and splits double helical DNA into single strands, increasing the absorbance. Most intercalators increase the melting temperature of DNA and also elongate the DNA chain.

Groove binders do not affect DNA chain length; hence, their binding does not change the melting point. Fig. 8 illustrates the impact of temperature on *ct*-DNA and its APB complex. The midpoint of inflection of the absorbance value showed the melting temperature. The melting temperatures of *ct*-DNA and APB were 72 ± 3 and 72 ± 3 ºC, respectively. The absence of a notable variation in the melting temperatures of *ct*-DNA and its complex indicates the lack of intercalation.

Interaction studies with potassium iodide (KI): Drug-DNA binding interactions may be better understood using iodide ions [51,52]. Ion interactions make negatively charged iodide ions universal quenchers. Absorption analyses were conducted to examine the effects of KI on APB absorption in the presence and absence of *ct*-DNA. DNA backbone phosphate ions oppose negatively charged iodide ions, hence iodide ions cannot easily reach intercalators. The unbound molecule interacts more with iodide ions than the intercalated molecule. However, groove binders are different (open), therefor iodide ions should interact similarly with free and bound molecules. The relative accessibility of APB to iodide was evaluated by UV-vis spectroscopy after the successive KI additions with and without DNA. As KI concentration increases, APB and the APB-*ct*-DNA complex absor-bance changes (Fig. 9). The absorption properties of both are nearly identical and the absence of substantial alteration in the absorption characteristics of the APB-*ct*-DNA complex with increasing KI concentration confirms a groove binding mode rather than an intercalation process.

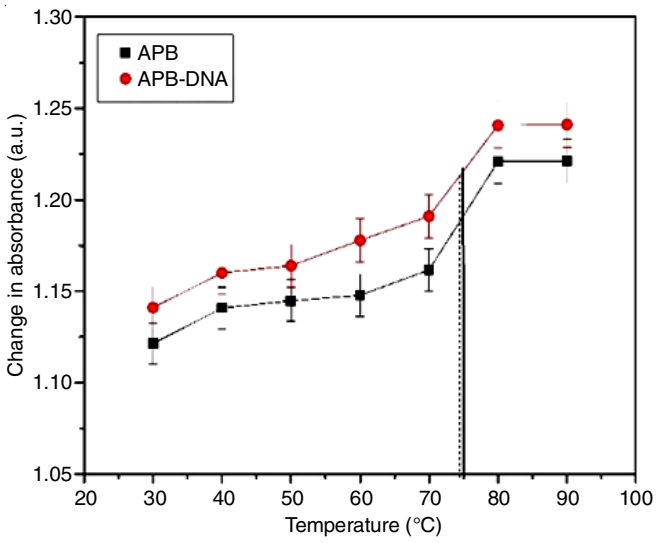

Fig. 8. Melting curve of 50 µM *ct*-DNA in the absence and presence of 50 µM APB with increasing temperature (30–100 ºC)

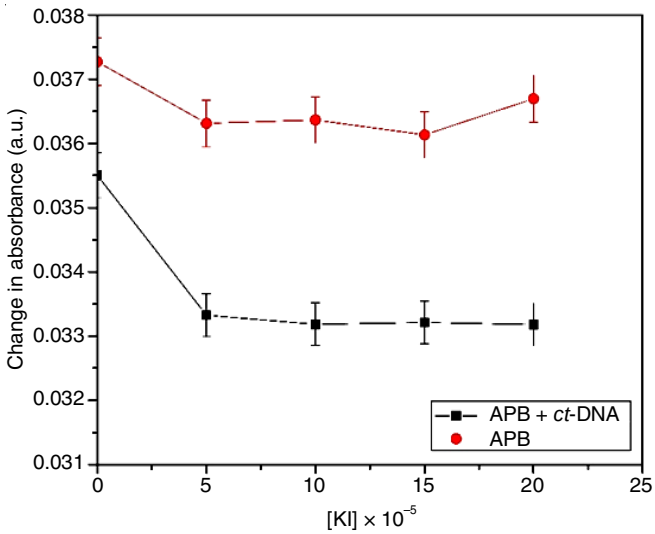

Fig. 9. Effect of KI on the binding of APB with *ct*-DNA. [APB] = 1 µM, [*ct*-DNA] = 1 µM, [KI] = 0-200 µM

Viscosity studies: The binding of APB to *ct*-DNA was further confirmed by the viscosity analysis. Intercalating drug molecules between DNA base pairs elongates the DNA chain and enhances the viscosity of the drug-DNA complex relative to pure DNA [18,53,54]. No impact is anticipated for DNA minor groove binding, and Fig. 10 illustrates the effect of APB concentrations on *ct*-DNA viscosity. Insignificant *ct*-DNA viscosity alterations with varying APB concentrations suggest groove binding by ruling out intercalation.

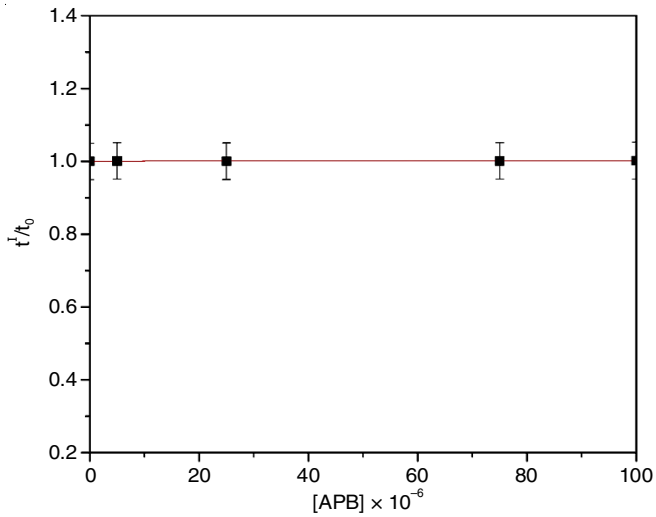

Fig. 10. Change in the viscosity of *ct*-DNA (100 µM) in the presence of APB (100 µM)

Effect of ionic strength in binding: Electrostatic or external binding, depending on ionic strength, occurs between the positively charged ligand and the negatively charged DNA backbone phosphate [40,54]. Increased ionic strength increases the quantity of counter ions (cations) in the media, decreasing the repulsion between negatively charged phosphate backbones and condensing DNA strands. Spectrum behaviour shows that the greater ionic strength lowers ligand-DNA binding. NaCl was used to determine solution ionic strength and its effect on binding. The absorbance of APB was measured with and without *ct*-DNA at different NaCl concentrations. Fig. 11 shows that minor electrostatic binding affects the absorbance behaviour of the complex at varying NaCl concentrations.

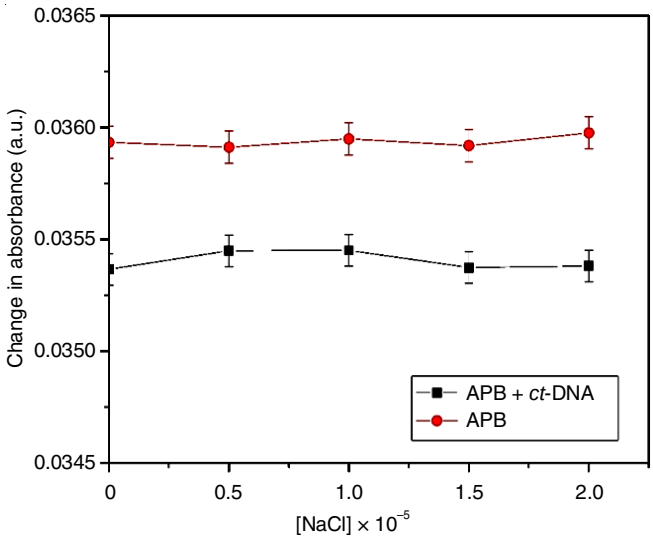

Fig. 11. Absorbance changes of APB and *ct*-DNA+APB, [APB] = 1 µM, [*ct*-DNA] = 1 µM, [NaCl] = 0-200 µM

Molecular docking studies: Fig. 12 shows APB docked in *ct*-DNA, aligning with minor groove binders in the DNA minor groove curvature. Table-2 compares the predicted binding free energy of the APB-*ct*-DNA system from docking studies to that of the HST-*ct*-DNA system (figure not shown).

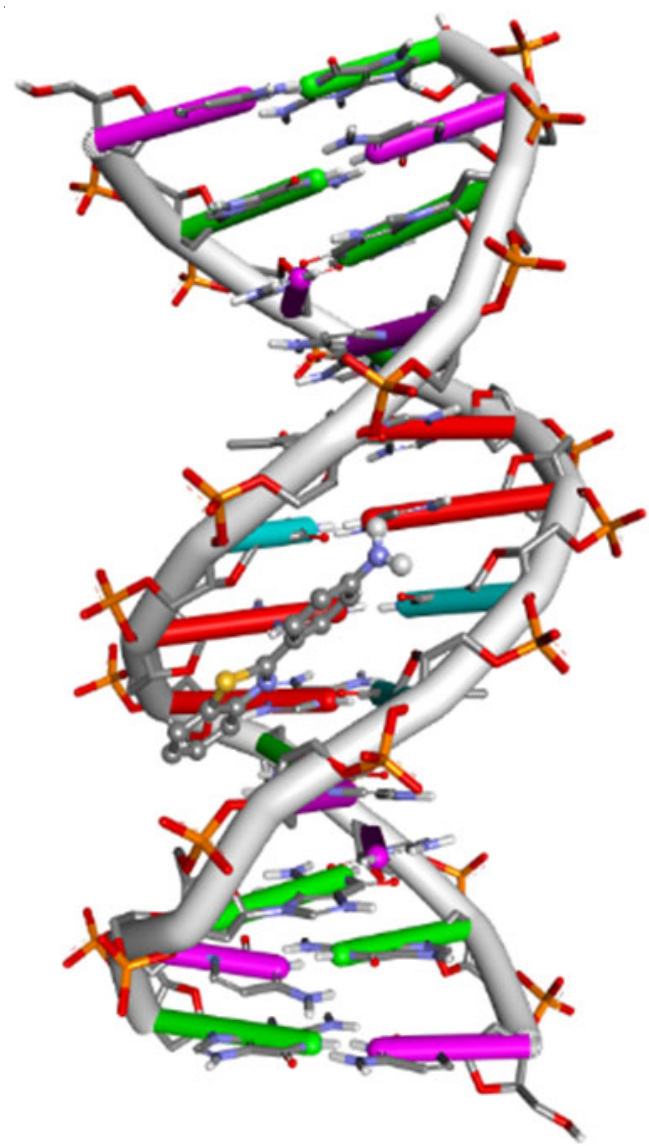

Fig. 12. Docked pose of APB in the minor groove of *ct*-DNA

TABLE-2
THEORETICAL FREE ENERGY CHANGE (kcal/mol) FOR APB-*ct*-DNA (453D) AND HST-*ct*-DNA BINDING (453D)*

Binding system	ΔG	E1	E2	E3
APB-*ct*-DNA	-8.18	-8.77	-0.01	-8.76
HST-*ct*-DNA*	-8.81	-10.01	+0.00	-10.01

ΔG is the estimated free energy of binding. E1 is the final intermolecular energy (E1 = E2 + E3). E2 denotes electrostatic energy. E3 is the sum of vdW + Hbond + desolv energy. *[Ref. 55]

The receptor interface residues involved in the interaction are shown in Table-3, derived from the ligplot (Fig. 13) and the 2D diagram (Fig. 14) of the complex generated from Discovery Studio. The residues DA 18(B) (adenine 18 of strand B) are at 2.17 as shown by the ligplot. The 2D image of the complex elucidates the participation of hydrogen bond formation between the nitrogen atom of APB and the residue DA (B18). The greater abundance of thymine residues next to the APB in the A–T region compared to the G–C region indicates a stronger binding affinity of the APB in the A–T region.

TABLE-3
THE AVERAGE DISTANCE BETWEEN RECEPTOR INTERFACE RESIDUES INVOLVED IN AN INTERACTION

Binding systems	Residues involved in the receptor interface (A and B stands for the DNA strand)	Bond length (Å)
APB-DNA	B: DA18 (H-bond)	2.12
	DT 19(B) (hydrophobic interaction)	–
	DT 7(A) (hydrophobic interaction)	–
	DC 9(A) (hydrophobic interaction)	–
	DT 8(A) (hydrophobic interaction)	–
	DG 10(A) (hydrophobic interaction	–
	DT 7(A) (hydrophobic interaction)	–
	DA 17(B) (hydrophobic interaction	–
	DT 20(B) (hydrophobic interaction	–

DA stands for adenine, DC for cytosine and DT for thymine.

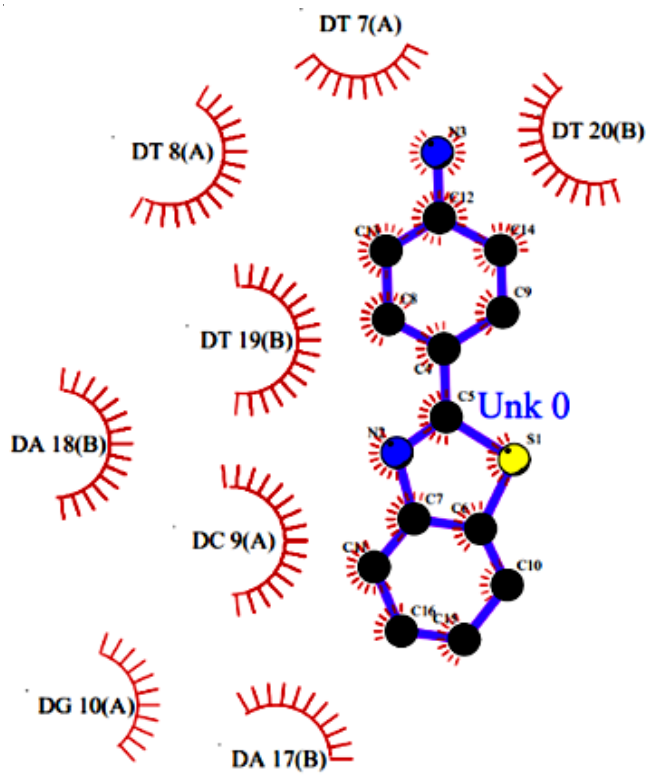

Fig. 13. The ligplot of APB-DNA complex

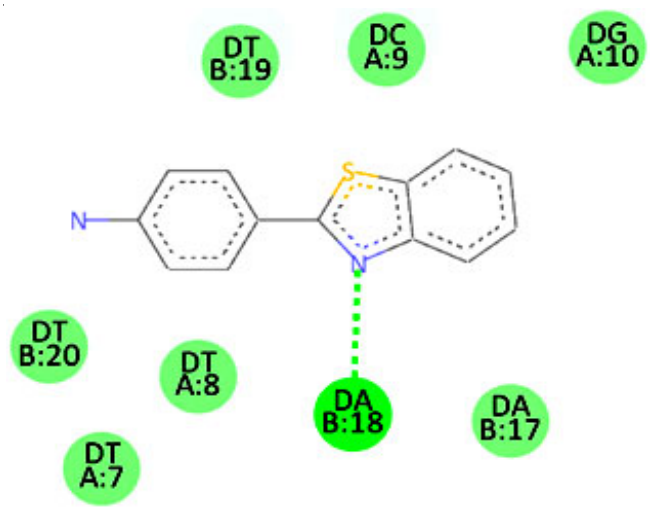

Fig. 14. 2D image of APB-DNA complex

Conclusion

The binding interactions of 2-(4-aminophenyl)benzothiazole (APB) and *ct*-DNA were investigated using various biophysical approaches. The quenching of APB fluorescence by *ct*-DNA was found to be dynamic. At 298, 303 and 308 K, APB-DNA binding constants were $1.0 \pm 0.2 \times 10^5$, $2.4 \pm 0.3 \times 10^5$ and $3.5 \pm 0.3 \times 10^5$, respectively and APB binds to the minor groove of *ct*-DNA, as demonstrated by marker displacement, viscosity and DNA melting examinations, however, the KI investigations supported the groove binding mode. Electrostatic external binding was non-existent, but the thermodynamic characteristics indicated the major role of hydrophobic forces in the interaction. Circular dichroism (CD) studies also revealed no structural alterations in *ct*-DNA following to APB interaction. Molecular docking images illustrated the actual and potential positions of APB within the minor groove of *ct*-DNA. The outcomes of this research may assist in developing human drug compounds. The findings may potentially facilitate the development of gene-based therapeutics by elucidating the interactions between chemicals and DNA sequences.

ACKNOWLEDGEMENTS

The authors express their gratitude to GITAM Deemed to be University, Hyderabad Campus for providing the research facilities. Ragaiahgari Srinivas Reddy acknowledges the support of B V Raju Institute of Technology, Hyderabad. Thanks, are also due to the Central Research Center, University of Hyderabad for providing the circular dichroism (CD) facilities.

CONFLICT OF INTEREST

The authors declare that there is no conflict of interests regarding the publication of this article.

REFERENCES

1. G.K. Prashanth, M. Gadewar, S. Rao, M.K. Ghosh, K.V. Yatish and M.M. Swamy, 2024, https://doi.org/10.1039/9781837674015-00086
2. N. Paoletti and C.T. Supuran, *Arch. Pharm.*, **357**, e2400259 (2024); https://doi.org/10.1002/ardp.202400259
3. A. El Alami, A. El Maraghi and H. Sdassi, *Synth. Commun.*, **54**, 769 (2024); https://doi.org/10.1080/00397911.2024.2337089
4. K.P. Yadav, M.A. Rahman, S. Nishad, S.K. Maurya, M. Anas and M. Mujahid, *Intelligent Pharm.*, **1**, 122 (2023); https://doi.org/10.1016/j.ipha.2023.06.001
5. R. Mahapatra, K. Hazra and J. Asian, *Res. Med. Pharm. Sci.*, **12**, 13 (2023); https://doi.org/10.9734/ajrimps/2023/v12i1206
6. R. Dubey, P.K. Shrivastava, P.K. Basniwal, S. Bhattacharya and N.S.H.N. Moorthy, *Mini Rev. Med. Chem.*, **6**, 633 (2006); https://doi.org/10.2174/138955706777435706
7. S. Teli, A. Sethiya and S. Agarwal, *Chemistry*, **6**, 165 (2024); https://doi.org/10.3390/chemistry6010009
8. P.C. Sharma, A. Sinhmar, A. Sharma, H. Rajak and D.P. Pathak, *J. Enzym. Inhib. Med. Chem.*, **28**, 240 (2013); https://doi.org/10.3109/14756366.2012.720572
9. A. Kamal, M.A.H. Syed and S.M. Mohammed, *Expert Opin. Therap. Patents*, **25**, 335 (2015); https://doi.org/10.1517/13543776.2014.999764
10. I. Hutchinson, M.-S. Chua, H.L. Browne, V.T. Tracey, D. Bradshaw, A.D. Westwell and M.F.G. Stevens, *J. Med. Chem.*, **44**, 1446 (2001); https://doi.org/10.1021/jm001104n

11. B. Mavroidi, M. Sagnou, E. Halevas, G. Mitrikas, F. Kapiris, P. Bouziotis, A.G. Hatzidimitriou, M. Pelecanou and C. Methenitis, *Inorganics*, **11**, 132 (2023); https://doi.org/10.3390/inorganics11030132
12. X. Li, Q. Ma, R. Wang, L. Xue, H. Hong, L. Han and N. Zhu, *Phosphorus Sulfur Silicon Relat. Elem.*, **197**, 689 (2022); https://doi.org/10.1080/10426507.2022.2033744
13. J. Sharma, P. Mishra and J. Bhadoria, *Results Chem.*, **4**, 100670 (2022); https://doi.org/10.1016/j.rechem.2022.100670
14. C. Kiritsis, B. Mavroidi, A. Shegani, L. Palamaris, G. Loudos, M. Sagnou, I. Pirmettis, M. Papadopoulos and M. Pelecanou, *ACS Med. Chem. Lett.*, **8**, 1089 (2017); https://doi.org/10.1021/acsmedchemlett.7b00294
15. M.M. Aleksic and V. Kapetanovic, *Acta Chim. Slov.*, **61**, 555 (2014).
16. M.M.V. Ramana, R. Betkar, A. Nimkar, P. Ranade, B. Mundhe and S. Pardeshi, *J. Photochem. Photobiol. B*, **151**, 194 (2015); https://doi.org/10.1016/j.jphotobiol.2015.08.012
17. M. Sirajuddin, S. Ali and A. Badshah, *J. Photochem. Photobiol. B*, **124**, 1 (2013); https://doi.org/10.1016/j.jphotobiol.2013.03.013
18. R. Hassan, A. Husin, S. Sulong, S. Yusoff, M.F. Johan, B.H. Yahaya, C.Y. Ang, S. Ghazali and S.K. Cheong, *Malays. J. Pathol.*, **37**, 165 (2015).
19. A. Minhas-Khan, M. Ghafar-Zadeh, T. Shaffaf, S. Forouhi, A. Scime, S. Magierowski and E. Ghafar-Zadeh, *Actuators*, **10**, 246 (2021); https://doi.org/10.3390/act10100246
20. M.M. Silva, E.O.O. Nascimento, E.F. Silva, J.X. Araújo, C.C. Santana, L.A.M. Grillo, R.S. de Oliveira, P. R.R.Costa, C.D. Buarque, J.C.C. Santos and I.M. Figueiredo, *Int. J. Biol. Macromol.*, **96**, 223 (2017); https://doi.org/10.1016/j.ijbiomac.2016.12.044
21. A. Usman and M. Ahmad, *Chemosphere*, **181**, 536 (2017); https://doi.org/10.1016/j.chemosphere.2017.04.115
22. Z. Mirzaei-Kalar, *J. Pharm. Biomed. Anal.*, **161**, 101 (2018); https://doi.org/10.1016/j.jpba.2018.08.033
23. A.C. Wallace, R.A. Laskowski and J.M. Thornton, *Prot. Eng. Design Select.*, **8**, 127 (1995); https://doi.org/10.1093/protein/8.2.127
24. Ö. Karaca, S.M. Meier-Menches, A. Casini and F.E. Kühn, *Chem. Commun.*, **53**, 8249 (2017); https://doi.org/10.1039/C7CC03074F
25. A.G. Cherstvy, *Phys. Chem. Chem. Phys.*, **13**, 9942 (2011); https://doi.org/10.1039/c0cp02796k
26. B.K. Sahoo, K.S. Ghosh, R. Bera and S. Dasgupta, *Chem. Phys.*, **351**, 163 (2008); https://doi.org/10.1016/j.chemphys.2008.05.008
27. M. Suganthi and K.P. Elango, *Phys. Chem. Liquids*, **56**, 299 (2018); https://doi.org/10.1080/00319104.2017.1329426
28. K.G. Fleming, Encyclopedia of Spectroscopy and Spectrometry, 2nd ed., Academic Press, edn. 2 pp 628-634 (2010); https://doi.org/10.1016/B978-0-12-374413-5.00357-2
29. S.B. Kou, J.Y. Lin, B.L. Wang, J.H. Shi and Y.X. Liu, *J. Mol. Struct.*, **1224**, 129024 (2021); https://doi.org/10.1016/j.molstruc.2020.129024
30. J.R. Lakowicz, Principles of Fluorescence Spectroscopy, Springer US, Boston, MA. USA (2006); https://doi.org/10.1007/978-0-387-46312-4
31. M. Zolfagharzadeh, M. Pirouzi, A. Asoodeh, M.R. Saberi and J. Chamani, *J. Biomol. Struct. Dyn.*, **32**, 1936 (2014); https://doi.org/10.1080/07391102.2013.843062
32. M. Mondal, K. Ramadas and S. Natarajan, *Spectrochim. Acta A Mol. Biomol. Spectrosc.*, **183**, 90 (2017); https://doi.org/10.1016/j.saa.2017.04.012
33. N. Shakibapour, F. Dehghani Sani, S. Beigoli, H. Sadeghian and J. Chamani, *J. Biomol. Struct. Dyn.*, **37**, 359 (2019); https://doi.org/10.1080/07391102.2018.1427629
34. S. Li, J. Pan, G. Zhang, J. Xu and D. Gong, *Int. J. Biol. Macromol.*, **101**, 736 (2017); https://doi.org/10.1016/j.ijbiomac.2017.03.136
35. M. Dareini, Z. Amiri Tehranizadeh, N. Marjani, R. Taheri, A. Talebi, S. Aslani-Firoozabadi, N. NayebZadeh Eidgahi, M.R. Saberi and J. Chamani, *Spectrochim. Acta A Mol. Biomol. Spectrosc.*, **228**, 117528 (2020); https://doi.org/10.1016/j.saa.2019.117528
36. P.V. Scaria and R.H. Shafer, *J. Biol. Chem.*, **266**, 5417 (1991); https://doi.org/10.1016/S0021-9258(19)67611-8
37. S. Latt and G. Stetten, *J. Histochem. Cytochem.*, **24**, 24 (1976); https://doi.org/10.1177/24.1.943439
38. S.U. Rehman, Z. Yaseen, M.A. Husain, T. Sarwar, H.M. Ishqi and M. Tabish, *PLoS One*, **9**, e93913 (2014); https://doi.org/10.1371/journal.pone.0093913
39. T.A. Wani, N. Alsaif, H.A. Bakheit, S. Zargar, A.A. Al-Mehizia and A.A. Khan, *Bioorg. Chem.*, **100**, 103957 (2020); https://doi.org/10.1016/j.bioorg.2020.103957
40. S. Kashanian, Z. Shariati, H. Roshanfekr and S. Ghobadi, *DNA Cell Biol.*, **31**, 1341 (2012); https://doi.org/10.1089/dna.2012.1662
41. K. Nejedlý, *Nucleic Acids Res.*, **33**, e5 (2005); https://doi.org/10.1093/nar/gni008
42. M. Vorlícková, *Biophys. J.*, **69**, 2033 (1995); https://doi.org/10.1016/S0006-3495(95)80073-1
43. J. Kypr and M. Vorlíèková, *Biopolymers*, **67**, 275 (2002); https://doi.org/10.1002/bip.10112
44. P. Uma Maheswari and M. Palaniandavar, *J. Inorg. Biochem.*, **98**, 219 (2004); https://doi.org/10.1016/j.jinorgbio.2003.09.003
45. V.I. Ivanov, L.E. Minchenkova, A.K. Schyolkina and A.I. Poletayev, *Biopolymers*, **12**, 89 (1973); https://doi.org/10.1002/bip.1973.360120109
46. S.S. Jain, M. Polak and V.N. Hud, *Nucleic Acids Res.*, **31**, 4608 (2003); https://doi.org/10.1093/nar/gkg648
47. J.L. Mergny, G. Duval-Valentin, C.H. Nguyen, L. Perrouault, B. Faucon, M. Rougée, T. Montenay-Garestier, E. Bisagni and C. Hélène, *Science*, **256**, 1681 (1992); https://doi.org/10.1126/science.256.5064.1681
48. S. Huang, Y. Liang, C. Huang, W. Su, X. Lei, Y. Liu and Q. Xiao, *Luminescence*, **31**, 1384 (2016); https://doi.org/10.1002/bio.3119
49. Y. Sun, T. Peng, L. Zhao, D. Jiang and Y. Cui, *J. Lumin.*, **156**, 108 (2014); https://doi.org/10.1016/j.jlumin.2014.07.014
50. L. Fin and P. Yang, *J. Inorg. Biochem.*, **68**, 79 (1997); https://doi.org/10.1016/S0162-0134(97)00004-4
51. C. Ji, X. Yin, H. Duan and L. Liang, *Int. J. Biol. Macromol.*, **168**, 775 (2021); https://doi.org/10.1016/j.ijbiomac.2020.11.135
52. K. Miskovic, M. Bujak, M. Baus Loncar and L. Glavas-Obrovac, *Arh. Hig. Rada Toksikol.*, **64**, 593 (2013); https://doi.org/10.2478/10004-1254-64-2013-2371
53. C. Sengupta and S. Basu, *RSC Adv.*, **5**, 78160 (2015); https://doi.org/10.1039/C5RA13035B
54. S. Tabassum, S. Amir, F. Arjmand, C. Pettinari, F. Marchetti, G. Lupidi, N. Masciocchi and G. Pettinari, *Eur. J. Med. Chem.*, **60**, 216 (2013); https://doi.org/10.1016/j.ejmech.2012.08.019
55. A.T.S. Bodapati, B.K. Sahoo, S.R. Ragaiahgari, L. Kandikonda and S.R. Madku, *Int. J. Biol. Macromol.*, **217**, 1027 (2022); https://doi.org/10.1016/j.ijbiomac.2022.07.177